Metastable Frenkel pairs and the W11–W14 electron paramagnetic resonance centers in diamond

J. P. Goss, M. J. Rayson, and P. R. Briddon
School of Natural Sciences, University of Newcastle upon Tyne, Newcastle upon Tyne NE1 7RU, United Kingdom

J. M. Baker
Oxford Physics, Clarendon Laboratory, Parks Road, Oxford OX1 3PU, United Kingdom

(Received 18 October 2005; revised manuscript received 14 March 2007; published 3 July 2007)

Diamond is a material that shows great promise for particle detection applications. However, under irradiation with energetic particles, many thermally stable defects are created, made up of lattice vacancies, self-interstitials, and complexes with impurities. Relatively distant Frenkel (vacancy–self-interstitial) pairs have long been used to explain optical and magnetic spectra in irradiated material. However, in diamond we show, using first-principles methods, that the ability of carbon to form sp^2-, sp^3-, and π-bonding configurations leads to particularly strong reconstructions between vacancy–self-interstitial pairs within a few atomic spacings of each other. The resultant complexes are anticipated to be optically and paramagnetically active, and we propose correlation of negatively charged Frenkel pairs with the W11–W14 paramagnetic centers, where substitutional nitrogen donors act as source of electrons and are not an intimate component part of the paramagnetic defects.

DOI: 10.1103/PhysRevB.76.045203 PACS number(s): 61.72.Ji, 61.72.Bb, 71.20.Mq, 71.23.An

I. INTRODUCTION

Diamond that has been irradiated with high energy electrons, neutrons, or gamma rays or subjected to ion implantation gives rise to characteristic optical and electron paramagnetic resonance (EPR) centers. In a number of cases, atomistic models have been assigned, including the most primitive centers: the isolated lattice vacancy (V) and self-interstitial (I).

The neutral and negatively charged V are detected optically (GR1 and ND1 bands at 1.673 and 3.149 eV, respectively),[1] with the negative charge state also being responsible for the S1 ($S=3/2$) EPR center.[2] I is also seen optically, giving rise to a complex optical spectrum[3,4] but the unambiguous identification of this center came from the R2, $S=1$ EPR spectrum.[5] The structure of I is shown schematically in Fig. 1(b).

V and I migrate thermally around 600 and 425 °C, respectively,[1,5] with associated activation energies of 2.3 and 1.7 eV. However, under ionizing conditions, I moves *athermally* forming multi-interstitial complexes, even at cryogenic temperatures.[6,7]

Aggregation of I (and V) is driven by the reduction in total-energy concomitant with the reduction in the number of dangling bonds (DBs). For instance, an EPR-active form of di-interstitial (I_2),[8] labeled R1 [made up from nearest-neighbor pair [001]-aligned self-interstitials, Fig. 1(c)], has two three fold-coordinated C atoms, the same number as I. This reduction of two DBs more than offsets the increase in strain energy.[9]

Calculations show that there is a more stable configuration of I_2: two puckered bond-centered self-interstitials on opposite sides of a hexagonal ring forming a π bond, Fig. 1(d). All atoms are chemically satisfied, and this diamagnetic, optically inactive form is 1.2 eV lower in energy than that responsible for R1.[3] The presence of R1 therefore represents evidence that metastable defects are produced during irradiation. Additionally, we note that it has been shown experimentally that there is a barrier to recombination of vacancies with self-interstitials in relatively N-free material,[7] which may also indicate metastability.

Recently, it was shown that complexes of nitrogen (N_s) and I reconstruct to form low-energy, metastable configurations tentatively correlated with defects in irradiated and annealed N-containing diamond.[10] In particular, N_s and I at second and third sites along a ⟨110⟩ chain have a considerably lower energy than the isolated components, but are higher in energy than interstitial nitrogen (N_i). The metastable complexes are mainly characterized by the introduction of π bonding and chemical reconstruction. It is also worthy of note that metastable Frenkel pairs with a considerable barrier to recombination have been proposed for graphite.[11]

Guided by these earlier results, we have now examined structures made up from Frenkel pairs separated by various distances.

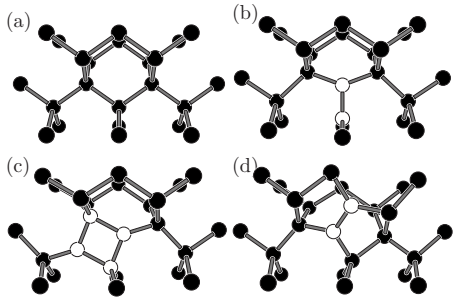

FIG. 1. Schematics of radiation products in diamond. (b) D_{2d}, [001]-oriented split interstitial, (c) C_{2h} metastable nearest-neighbor di-interstitial, and (d) π-bonded ground-state di-interstitial. Black and white circles represent the host and interstitial C atoms, respectively. A section of defect-free material is shown in (a) for comparison.

II. METHOD

Calculations were carried out using the local-spin-density-functional technique, implemented in the AIMPRO code.[12] To model the various defects, 64-, and 216-atom supercells have been used. The Brillouin zone is sampled using the Monkhorst-Pack scheme,[13] generally with a mesh of $2\times2\times2$ special k points. For representative cases, we have compared total energies with a $4\times4\times4$ mesh, and this suggests that our results from the smaller mesh are converged to of the order of 10 meV. Core electrons are eliminated by using norm-conserving pseudopotentials.[14]

The wave function basis consists of Gaussian functions centered at each atom.[15] For carbon, the basis functions are combinations of eight s- and p-Gaussian functions, with the addition of five d-Gussian polarization functions. For nitrogen, the basis consists of independent s, p, and d-Gaussians with four widths. The charge density is Fourier transformed using plane waves with a cutoff of 300 Ry, which yields total energies converged to around 1 meV. The lattice constant and bulk modulus of diamond using these bases are within ~1 and 5% respectively, of the experimental values, while the direct and indirect band gaps at 5.68 and 4.26 eV, respectively, are close to previously published plane-wave local density approximation values.[16]

The formation energy for system X in charge state q are calculated in the usual way using

$$E^f(X,q) = E(X,q) - \sum \mu_i + q(E_v + \mu_e) + \chi(q), \qquad (1)$$

where E is the calculated total energy, μ_i and μ_e are the chemical potentials of the atoms and electrons, respectively, E_v is the energy of the valence band top, and χ is the correction for periodic boundary conditions, for which we include only the Madelung term,[17] which for cubic supercells of side lengths $2a_0$ and $3a_0$ are around $0.53q^2$ and $0.35q^2$ eV, respectively.

Donor or acceptor electrical levels are not estimated using the formation energies, but instead by comparison of the ionization potential or electron affinity of a bulk supercell,[15] as suggested previously,[18] and discussed in detail for application to defects in diamond.[19]

The methodology for calculating spin-spin components of the zero-field-splitting tensor, D, has been presented elsewhere.[3,20] In the results presented in this study, we calculate D using the Kohn-Sham functions of the n highest occupied bands at Γ for $S=n/2$. This approach has proved successful for centers in diamond.[3,20] The calculated values do not include spin-orbit contributions, but these are expected to be small in diamond. Previous calculations suggest that the calculated values are typically the correct order of magnitude, and often within tens of percent. Tensor-component directions relative to crystallographic directions are generally well reproduced.

Localized vibrational modes (LVMs) are calculated by obtaining second derivatives of the total energy with respect to the atom positions for a subset of atoms (typically the defect atoms and their immediate neighbors). The dynamical matrix is then made up from a combination of these explicitly calculated terms and ones obtained from a valence-force potential for the remaining atoms.[21]

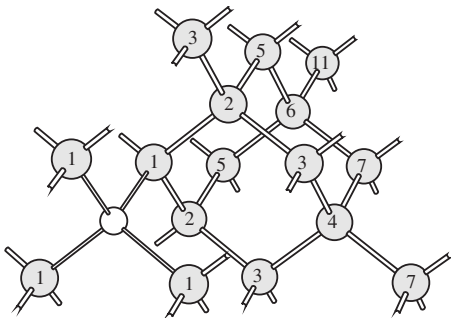

FIG. 2. Schematic illustration showing the neighboring sites of the vacancy (white circle). The numbers indicate the concentric shell to which the gray carbon atoms belong.

We use the convention that a positive binding energy implies that the reaction $A+B\rightarrow AB$ is exothermic.

One question that may arise with our methodology is the role of many body effects. Our calculations include electron-electron correlation in the approximation of spin polarized density-functional theory. It is generally accepted that this treatment cannot correctly describe certain systems, a key example being the neutral vacancy with a one-electron configuration t_2^2 which yields several multiplet states split by the order of eVs.[22] Indeed, the GR1 optical band arises from a transition between different multiplet states which can predominantly be derived from the same t_2^2 one-electron configuration. These effects are typically important for systems of high symmetry with partially occupied states at the Fermi level, or where occupied and empty levels not related by symmetry are close in energy. Under such circumstances, the ground-state spin state may not be obtained with certainty. However, in favorable circumstances, the above approach may still be used to determine specific properties of defects using a procedure devised by von Barth.[23] For instance, the $S=3/2$ ground-state configuration of $V^-(t_2^3)$ is of a different symmetry from the singlet configurations and one can reasonably expect the spin-density and derived properties to be sufficiently accurate. The von Barth formalism has previously been successfully used to reproduce the ND1 (3.149 eV) optical transition of V^-,[24] and multiplets of the negatively charged vacancy-nitrogen complex.[25]

Indeed, zero-field splittings for several multiplet systems have been calculated previously based upon these principles. For instance, the spin-triplet states of mono-, di- and tri-self-interstitial complexes are reproduced to a reasonable accuracy,[3] as is that of the W15 EPR center, the $S=1$ configuration of the negatively charged vacancy-nitrogen complex.[26]

III. NATIVE FRENKEL PAIRS

We relaxed $V\cdots I$ pairs separated by a range of host sites. The shells of atoms surrounding the vacant site are shown schematically in Fig. 2. In each of the first six shells, we have relaxed the distinct orientations of the [001] split interstitial.

TABLE I. Formation energies for Frenkel pairs in diamond (eV). The donor and acceptor levels (eV) are referenced to above the valence band maximum and below the conduction band minimum, respectively. The value for the infinitely separated pair is taken from the sum of values in Refs. 3 and 22. The results marked by * indicate that they have been taken from the 216-atom cubic supercell calculations.

		E^f (eV)				
Neighbor	Symmetry	+1	0	−1	(0/+)	(−/0)
BD	C_{2h}		7.8			
2	C_1	Unstable		19.0		
2	C_s	15.9	16.7	18.9	1.7	3.0
3	C_1	18.3	19.0	20.1	1.6	3.0
3	C_s	Unstable		20.5		
4*	C_2	17.3	18.8	20.8	2.1	2.7
4*	C_{2v}	17.3	18.7	20.6	2.0	2.8
5	C_1	15.8	16.5	18.7	1.6	3.0
5	C_s	15.8	16.5	18.6	1.6	3.0
6*	C_1	17.7	18.8	20.9	1.6	2.6
6*	C_s	17.3	18.8	20.8	2.1	2.7
∞			18.3			

A. Formation energies and electrical levels

To facilitate comparison with the energy scales for isolated native defects as well as pristine diamond, we present the formation energies of the Frenkel pairs in Table I, with $\mu_e=0$ eV in Eq. (1). Relaxed planar second- and fifth-neighbor pairs in the 216-atom supercells yield formation energies within 0.1 eV of those presented for the 64-atom supercells, with electrical levels agreeing to within the same margin.

Some initial configurations (e.g. nearest neighbor) annihilate or form a bond defect[27] (BD) shown in Fig. 3(b). However, of interest are sites in the second and fifth concentric shells around the vacancy, shown in Figs. 3(c)–3(f), all of which show reconstruction similar to previously found for $N_s\cdots I$ complexes.[10] These defects have four DBs: one on an interstitial component (gray atoms, Fig. 3) and three on V. This corresponds to a reduction of two DBs relative to separated Frenkel pairs (where there are two on I and four on V).

All other neutral systems we examined had formation energies of around 19 eV (see Table I) and no obvious reconstructions, suggesting that in these cases the component parts are only weakly interacting and may be considered as being dissociated.

B. Electronic structure

We now turn to the electronic properties. As alluded to above, the reconstructed defects can be considered as being comprised of four DBs: a vacancy component with three nearly equal DBs plus a single DB on the interstitial. This means that there are several possible spin configurations for each geometric arrangement.

Where Frenkel pairs were structurally stable in the neutral charge state, $S=1$ and $S=0$ states are too close in energy to determine with any certainty which is the ground state. Where the constituents chemically reconstruct $S=2$ is always more than 1 eV higher in energy. However, $S=2$ is the ground state for nonreconstructed pairs.

When N-doped diamond is in thermodynamic equilibrium, Frenkel pairs should be negatively charged, since their acceptor levels (Table I) are considerably lower in the band gap than the N donor level. In this charge state, the reconstructed pairs marginally favor a $S=3/2$ spin state, corresponding to $S=1/2$ on the interstitial in parallel with $S=1$ on the vacancy. Nonreconstructed pairs favor a $S=5/2$ configuration, corresponding to the R2 and S1 EPR centers. In the positive charge state, $S=1/2$ is preferred, with $S=3/2$ being competitive for nonreconstructed pairs.

The gap states of the Frenkel pairs, as well as admitting the possibility of paramagnetic activity, suggest that they should be optically active. Figure 4 shows the location of gap levels for the four negatively charged reconstructed Frenkel pairs. Although it is crude, one can estimate a transition energy by finding the difference in energy between filled and empty Kohn-Sham levels localized on the defects, yielding values in the range 2.3–3.1 eV for the reconstructed Frenkel pairs. The gap states for the four configurations have a common origin. The lowest, fully occupied level around E_v is relatively delocalized, with a contribution from the π-bonding reconstruction and a bonding combination of the sp orbitals on the three DBs on the vacancy component. The three midgap levels are combinations of the p orbital on the threefold component of the self-interstitial (gray atoms, Fig. 3) and antibonding combinations of sp orbitals on the three DBs of the vacancy. The empty level high in the band gap has a component of π^* at the reconstruction.

An analysis of the localization of the gap levels for the four metastable structures supports the view that there is a chemical rebonding between the two structural components.

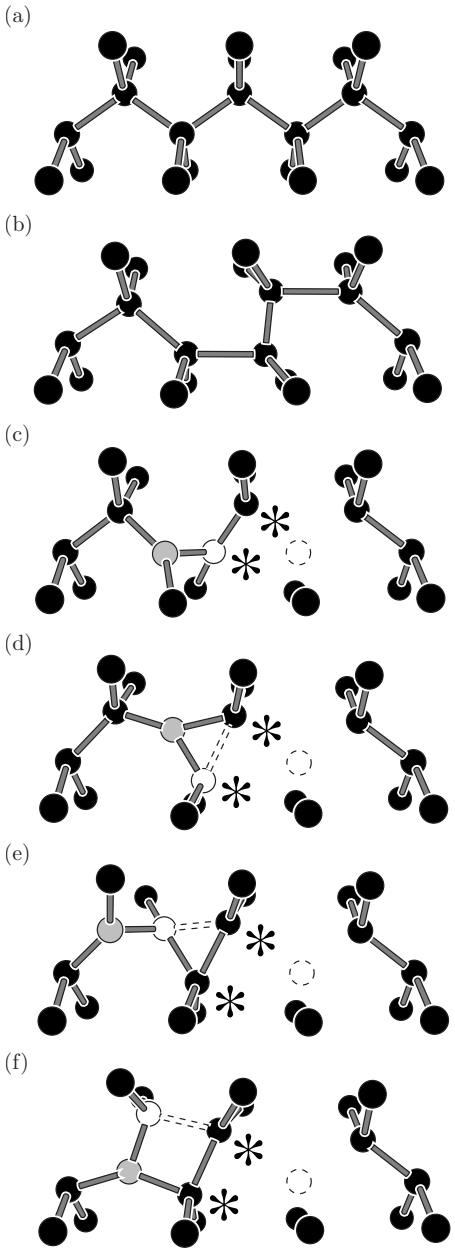

FIG. 3. Schematic structures of native Frenkel-pair defects in diamond. (b) is the C_{2h} metastable bond defect, (c) and (d) are the C_1 and C_s symmetry second-neighbor pairs, and (e) and (f) are the C_1 and C_s fifth-shell pairs. (a) shows a section of bulk material for comparison. Black, gray, and white circles represent the host atoms, threefold-coordinated interstitial atoms, and reconstructed interstitial atoms, respectively, with dashed white circles indicating the vacancy sites in (c)–(f). Dashed bonds indicate reconstructions, and asterisks indicate schematically the location of the p lobes that form the π bond.

C. Vibrational modes

Given that there is an interstitial component of the defects, it is highly likely that they would give rise to LVMs. Indeed, many optical centers such as 3H, 5RL, and TR12 show a rich array of sidebands in the 1500–2000 cm^{-1} range[28–31] characteristic of those calculated for self-interstitials, their aggregates, and complexes.[3,10,24] Therefore, to give a more complete analysis of our defect structures, we have also calculated the LVMs, and the results are listed in Table II. The vibrational modes are made up from stretches between the two interstitial atoms and their neighbors, and would all be infrared and Raman active. Additionally, they may appear as local-mode replicas of optical transitions. For the planar structures, all modes reported in Table II transform under the A' irreducible representation.

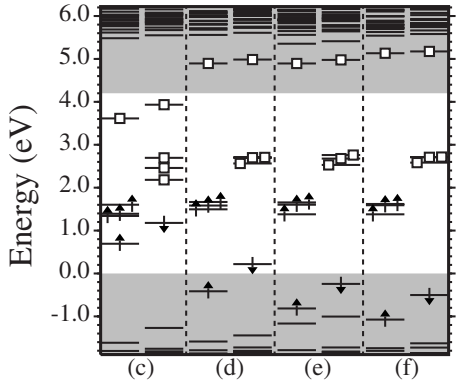

FIG. 4. Kohn-Sham eigenvalues for the reconstructed Frenkel pairs as labeled in Fig. 3. Shaded areas indicate the theoretical band gap, with E_v defined at 0 eV. Arrows indicate localized occupied levels and their spins, and white square the empty localized levels.

D. Barriers to interconversion

The formation of reconstructions within nearby self-interstitial–vacancy pairs may indicate a barrier to annihilation.

We have performed calculations to determine the energy required to convert the various forms of Frenkel pairs. We note that the migration of I proceeds via a reorientation,[3,24] and it seems likely that interconversion between structures in Fig. 3 would proceed in the same fashion. Of all the paths we have examined, one path seems more favorable than others, with (e)–(d) from Fig. 3 being around 1 eV. The nature of

TABLE II. Calculated vibrational modes of Frenkel pairs in diamond (cm^{-1}). For each mode, the frequency is also given where the isotope of the threefold-coordinated interstitial atom is substituted with ^{13}C or ^{15}N, as appropriate.

		$I\cdots V$, $q=-1$, $S=3/2$		
(c)	1579(1549)	1720(1707)	1851(1825)	
(d)	1380(1377)	1586(1570)	2166(2111)	
(e)	1371(1371)	1547(1536)	1590(1567)	1836(1802)
(f)	1388(1387)	1596(1566)	1884(1843)	
		$N_i\cdots V$, $q=-1$, $S=1$		
(c)	1508(1484)	1731(1715)	1844(1830)	
(d)	1394(1391)	1585(1568)	2099(2056)	
(e)	1414(1414)	1491(1470)	1578(1575)	1812(1785)
(f)	1394(1392)	1537(1513)	1837(1805)	

TABLE III. Binding energies for nitrogen bound at Frenkel pairs in diamond, given for the reaction N_s +Frenkel pair$\rightarrow N_i - V$. The donor and acceptor levels (eV) are referenced to above the valence band maximum and below the conduction band minimum, respectively.

		E^b (eV)			
Neighbor	Symmetry	0	−1	(0/+)	(−/0)
2	C_1	4.6	5.6	1.4	3.2
2	C_s	4.9	5.9	1.4	3.2
5	C_1	4.5	5.4	1.5	3.1
5	C_s	4.8	5.8	1.4	3.2

calculations for diffusion barriers involves the determination of saddle points in the total-energy surface as a function of geometry. However, the saddle point is not necessarily that with then lowest energy. Thus, although there may be other migration trajectories with different barrier heights, we find that other conversions require more energy, with an estimate for conversion between (c) and (f) being close to or above 3 eV. The barrier to dissociation (i.e., separation of the vacancy and interstitial components beyond the range of reconstruction) has also been estimated, and one mode of dissociation of structure (f) is around 3.5 eV. This is in agreement with the sum of migration barrier for self-interstitial migration (1.6–1.7 eV) (Refs. 32 and 33) and the binding energy of structure (f) (1.9 eV, Table I).

We shall return to these values later in this paper.

IV. N_I-V PAIRS

The reconstruction of Frenkel pairs results in a threefold-coordinated site particularly apt for incorporating of trivalent nitrogen. The most obvious sites are those indicated by the gray atoms in Figs. 3(c)–3(f). The remaining DBs in the vacancy component give rise to a pair of levels in the band gap, and in the negative charge state this corresponds to a potentially paramagnetic, $S=1$ system. Indeed, this is the case in our calculations with the $S=0$ state being around 0.2 eV higher in energy in all structures.

As can be seen from the data in Table III, the total energies are such that Fig. 3(d) is around more stable than Fig. 3(c), which is more stable than Fig. 3(e), the energy differences being 0.1–0.2 eV.

The band-gap states are shown in Fig. 5, and they closely follow those of the Frenkel pairs above. The main difference is that the interstitial-related orbital, previously close in energy to those from the vacancy (Fig. 4), is much lower in energy and approximately independent of structure (around $E_v+0.4$ eV) as it arises from the lone pair on the N atom.

As with the N-free complexes, these centers are expected to be optically active, with the Kohn-Sham eigenvalues suggesting electronic transitions in the range of 2.4–3.4 eV.

Finally, we also report the calculated LVMs of the $N_i \cdots V$ pairs (Table II).

V. W11–W14 EPR CENTERS

It is important where possible to relate calculations to available experimental data. As isolated I migrate at a lower temperature than isolated V, one might expect Frenkel pairs to recombine or dissociate at around the temperature for migration of I (400 °C). Hence, we seek defects whose concentrations change upon annealing in this region. A group of probably inter-related defects is seen in irradiated material containing N_s which undergo changes in this temperature range. These four centers, labeled W11–W14, are present in material irradiated at room temperature.[34] The spin states may be a matter of debate,[35] but the current data support $S=3/2$ for all four centers. The changes in concentration of these centers on annealing to successively higher temperatures[36,37] suggest that they are inter-related. Reference 36 records only EPR line heights, but the data are fairly consistent with those of Ref. 37, who recorded the concentrations of the defects. Both show concentrations of approximately 4:2:2:1 for |W11|:|W12|:|W13|:|W14| in room-temperature irradiated samples. This is also consistent with the data of Iakoubovskii *et al.*[38] who gave |W11|:|W13| as just over 4:2.

Both Refs. 36 and 37 note a drop in |P1|, the neutral substitutional nitrogen center,[4] on irradiation and a partial recovery upon annealing to ~400 °C, but precise concentrations are not recorded. However, as |P1| is greater in as-irradiated material than the sum of the concentrations of the W centers, and Ref. 36 shows a fourfold increase in |P1| on annealing to ~400 °C, the increase in |P1| at 400 °C appears to be considerably larger than the total loss of concentration

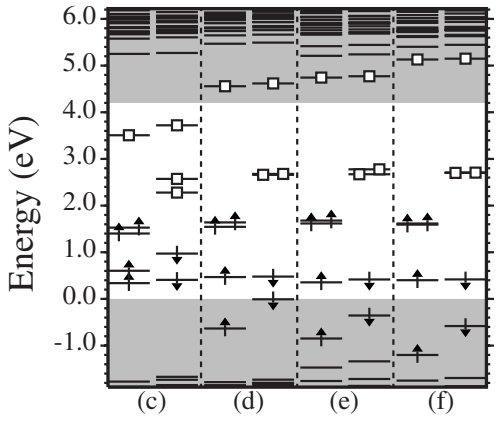

FIG. 5. Kohn-Sham eigenvalues for the negatively charged, $S=1$ N-containing reconstructed Frenkel pairs as labeled in Fig. 3. Shading and symbols as in Fig. 4.

of W centers. This does not necessarily imply a causal relation as other charge transfer processes are probably occurring in this temperature range, but it is consistent with the assumption in Ref. 37 that by some mechanism the W centers are finally converted into P1, by a thermally activated interconversion W11→W13→W14→P1. The role of W12 is uncertain: the decay of W11 appears to branch into W12 and W13, but the mode of decay of W12 is unclear.

Although W11–W14 are produced by irradiation of only type Ib diamond, the EPR data do not make clear the role of nitrogen, whether it forms part of the defect structure or acts merely as an electron donor: the EPR spectrum shows no resolved hyperfine structure ($A<2$ MHz). So the conversion of W14 to P1 above does not necessarily imply that W14 becomes P1, merely that the annealing out of W14 and the annealing in of some P1 are correlated.

There has also recently been some discussion as to the relationship of these centers to optical transitions, which are tentatively assigned to Frenkel pairs.[38] Zero-phonon lines at 2.367 and 2.535 eV have been associated with W11 and W13, and in this work it has been suggested that the transformation of the centers involves the incremental increase in separation of the V and I components, driven by an elastic repulsion between the centers. A feature, unique to irradiated material containing N_s, and of relevance to Frenkel pairs, is that V^- is observed: V possesses an acceptor level at $E_c-2.65$ eV,[39] which lies below the donor level of N_s, usually quoted as $E_c-1.7$ eV.[40] It is suggested that V^- has a larger dilation effect than V^0, potentially explaining why immediate recombination is suppressed in n-type material.[38] Neither of Refs. 36 and 37 record the concentrations of V^-, V^0, or I, but Fig. 1(a) of Ref. 38 shows an increase in $|I|$ and $|V^-|$ in electron-irradiated material ~4 units on annealing to 400 °C compared to an initial value for $\{|W11|+|W13|\}\sim 9.5$ units. Adding the initial values of $|W12|$ and $|W14|$ suggested by the ratios found[36,37] leads to a total initial as-irradiated concentration of W centers ~14 units. So these data are consistent with the suggestion that around 30% of the W centers may be converted to $(I+V^-)$ on annealing. Additionally,[38] γ irradiation produces W centers in preference to isolated V^-, which would be consistent with a relatively high probability of retaining the I close to the V in the relatively low energy displacements. In this model, the role of N_s is just as a remote electron donor to form V^-.

An alternative model has been proposed for W11–W14 as a distorted V^- center in which N_s is simultaneously the source of the negative charge and the geometric perturbation required for the low symmetries.[34] In this previous theoretical study, the distorted V^- system was modeled by using a set of empirical parameters describing strain, one electron, and exchange. They were able to explain the zero-field splittings of the W11–W14 centers. However, such an approach is problematic due to the relative freedom to choose parameters: this approach was used to link the R2 EPR center and 1.685 eV optical transition to a perturbed neutral vacancy,[41] but later evidence has shown unambiguously that R2 is the neutral self-interstitial.[5]

Nevertheless, the proposition of V^- perturbed by N_s is a current model. N_s^0 is paramagnetic (responsible for the P1 EPR center), and has a single dilated ⟨111⟩ bond, rendering it C_{3v} in symmetry.[42] The orientation of N_s^0 and its location relative to V^- yield $N_s^0\cdots V^-$ defects with different symmetries, consistent with W11–W14. However, there are serious problems with this model: (i) the lack of observed ^{14}N hyperfine interaction for W11–W14 is inconsistent with a complex related to the N_s^0 EPR center P1 [$A\sim 100$ MHz (Ref. 42)]; (ii) if N_s is close to V it could donate its unpaired electron yielding V^- and N_s^+. Now, isolated N_s^+ does not have a dilated bond, but instead is *tetrahedral*, as is V^-. The combination of two tetrahedral centers at various nearby distances will generally yield planar or higher symmetry. These would not be candidates for Jahn-Teller effects and it seems likely that $N_s^+\cdots V^-$ would not result in the observed low symmetry distortions. Indeed, we shall show later that this is what we find.

However, one would expect a much larger perturbation of V^- from a nearby I than from N_s^+, since I exerts a considerable strain on the surrounding material.[9]

All of the proposed models for W11–W14 involve V^-. This suggests that there might be analogous centers involving V^0 in irradiated N_s-free material. There are three $S=1$ centers, labeled A1, A2, and A3,[43,44] produced in irradiated Ia and IIa diamonds, which are also stable to only modest temperatures and have rather low symmetries. These are never seen in type Ib material, and it seems plausible that they are neutral charge states of three of the W centers. The annealing sequence has been much less thoroughly studied than that of the W centers, but appears to be A3→A2→A1 in the same region of temperature as the changes in the W centers. In contrast to the W11–W14 centers, A2 undergoes a motional averaging at temperatures above 300 K yielding orthorhombic symmetry (C_{2v}).

In order to assess the existing models for these centers against our favored proposal that they arise from native-defect pairs, we now present the results of the calculations of strained V^- and N_s-V pairs for W11–W14, and examine how well each fits the experimental data.

A. V^- under strain

[111] strain is simulated by deforming the supercells such that the cubic lattice vectors, (1,0,0), (0,1,0), and (0,0,1) become $(1+\varepsilon,\varepsilon,\varepsilon)$, $(\varepsilon,1+\varepsilon,\varepsilon)$, and $(\varepsilon,\varepsilon,1+\varepsilon)$, respectively, with ε positive and negative for tensile and compressive strains, respectively. The effect of the strain on V is shown schematically in Fig. 6.

In line with the model of Coulson and Kearsley,[45] we obtain a triply degenerate level in the middle of the band gap, and the $S=3/2$ effective spin of the negative charge state corresponds to the $^4A_2$ multiplet symmetry. The application of [111] strain splits this t_2 level into e and a_1 transforming under the C_{3v} point group, with the $S=3/2$ spin state having $^4A_2$ symmetry. The order of the two one-electron branches is dictated by the sense of the strain. Nominally, one can view these split levels as arising from groups of three DBs (e) and one DB (a_1) rendered nonequivalent by the perturbation. The splitting is plotted in Fig. 6. We find that the effect of strain on the electronic structure is relatively modest with splittings of less than half an eV for rather high strains.

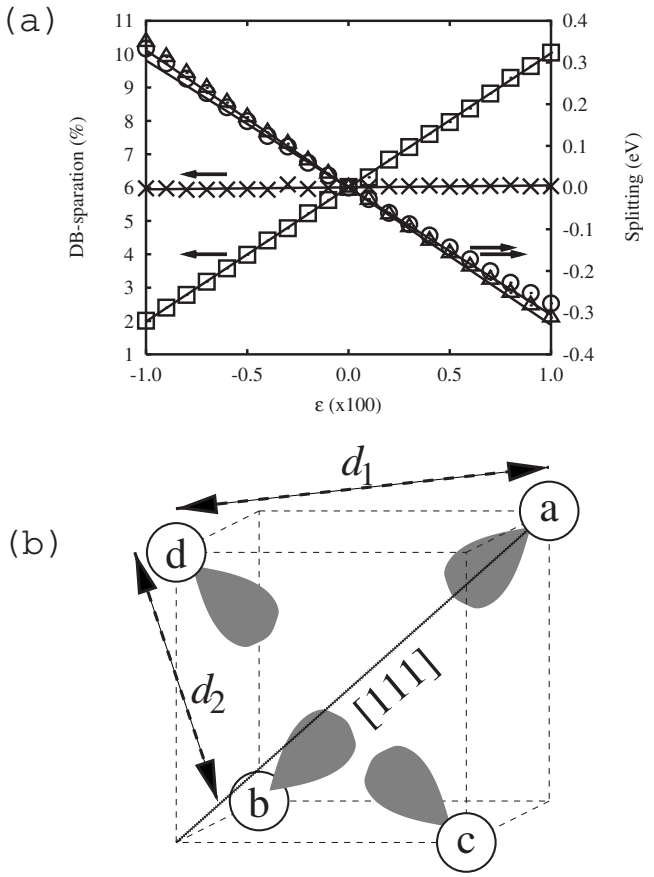

FIG. 6. Schematic of V^- under [111] strain. (a) shows the Kohn-Sham splitting $[E(e)-E(a_1)]$ and geometric variables, as indicated in (b), versus applied strain, ε. Circles and triangles show the splittings for the up and down spin polarizations, respectively. Squares and crosses show the fractional increase in the C-C distances d_1 and d_2 relative to the bulk second-neighbor separation, $a_0/\sqrt{2}$.

Estimates of the zero-field splitting for a [111] strained negatively charged vacancy of 61ε MHz suggest a very small magnitude even for large strains, and certainly much lower that the W11–W14 centers.[46] It seems likely that strain alone cannot be responsible for the EPR centers.

B. Neutral $N_s\cdots V$ complexes

We simulated $N_s^+-V^-$ pairs, with the two components at various distances. For the case where they are separated along a ⟨110⟩ host chain by two atomic sites, we find the neutral system having an effective spin of 3/2. There are no other gap states in the vicinity of those arising from the vacancy, and thus no other $S=3/2$ electronic configurations will be of any importance. The geometry of V^- is perturbed only slightly from the ideal T_d symmetry: all C-C distances are within 0.3% of the zero-strain point in Fig. 6. The proximity of N splits the t_2 level of the vacancy into three bands, which at the Brillouin-zone center lie separated by 280 and 40 meV. Indeed, despite the monoclinic symmetry, the orbitals can be closely correlated with those expected for the trigonally distorted vacancy with the a_1 level lying around 0.3 eV below e. This corresponds to a [111] compressive strain of $\varepsilon\sim 1\%$, much greater than the geometric perturbation would suggest. This weak splitting effect is also seen for N at other sites which is consistent with an on-site N_s^+. We find that the neutral $N_s\cdots V$ complexes in the first six shells (Fig. 2) are all planar or higher in symmetry.

In favor of a $N_s\cdots V$ model for W11–W14, they have a spin density with very little amplitude on the N atom as the levels involved are predominantly localized on the carbon DBs, consistent with the lack of observed ^{14}N hyperfine interaction for the W11–W14 EPR centers. The electronic localization and gap states render these complex candidates for the W11–W14 EPR centers.

However, it is not clear how to assign exactly four specific centers with either C_1 or C_s symmetry nor how to correlate these centers with the optical analogs.[38] Nor is it clear what the thermally activated process for the loss of these centers may be since V is not mobile.

C. Frenkel pairs

Since the properties of the Frenkel pairs have already been discussed above, we present here an assessment of the fit for these systems to the W11–W14 EPR centers.

First, the fact that negatively charged Frenkel pairs can be considered to be a single I site with $S=1/2$ and a V with $S=1$ would be consistent with the relatively small zero-field splittings seen in the W11–W14 EPR centers. Our results are therefore in line with the suggestions of Iakoubovskii *et al.*[38] that the role of N_s is as a remote electron donor, and that the centers correspond to negatively charged Frenkel pairs.

Second, there are exactly four stable systems, two with planar symmetry and two triclinic systems, corresponding to the experimental observations. Furthermore, the symmetries of the EPR centers increase in thermal stability in an order which fits rather well with the ordering of the total energies of the reconstructed pairs with $E(\mathrm{f})<E(\mathrm{e})<E(\mathrm{d})<E(\mathrm{c})$.

The formation of reconstruction within nearby self–interstitial-vacancy pairs and the associated barriers to interconversion or annihilation may account for the thermal stability of the W11–W14 EPR centers of up to 425 °C, corresponding to a modest enhancement over that of the isolated self-interstitial.

The calculations also tie in with the initial stages of annealing, which may be viewed as converting (e) into (c) and (d) into (f), or indeed via loss of (c) via annihilation. This decreases the concentration of triclinic centers, in line with experiment. The conversion of (d) into the more stable (f) has a relatively high energy barrier and will most probably compete with the loss of (d) via pair annihilation. We note that once one of the metastable forms have been created, dissociation is unlikely at moderate temperatures since the loss of the reconstruction (i.e., the formation of more DBs) cost around 2 eV plus an activation barrier.

It is important to consider the impact upon the nitrogen donor during the production and annealing of the Frenkel pairs. When W11–W14 are produced by irradiation, there is a large decrease observed in the concentration of N_s^0, consistent with the formation negatively charged centers via charge transfer. When W11–W14 have annealed out, there is an in-

crease in concentration of N_s^0 suggesting that on annihilation many of these centers lose their negative charge, as one would expect when I and V^- recombine. An increase in the concentration of I may indicate that also some of the W11–W14 centers dissociate on annealing, although the calculated energy required for this process is rather high. However, the experimental picture is completely consistent with a model for W11–W14 where N_s purely acts as a source of charge.

Thirdly, the electronic structure of the native Frenkel pairs (Fig. 4) fits reasonably well with the 2.367 and 2.535 eV zero-phonon lines associated with W11 and W13,[38] although a quantitative analysis is strictly beyond the scope of the method employed.

Finally, although the EPR spectra of the A1–A3 centers produced by irradiation of type Ia and IIa materials have been thoroughly investigated and interpreted in terms of spin Hamiltonian parameters, the details of their annealing behavior are less well known than those for W11–W14 defects. The fact that structure (c) is unstable in the neutral charge state would be consistent with the presence of three rather than four $S=1$, neutral EPR centers, as are the symmetries. We conclude that although the fit is imperfect, there is circumstantial evidence to associate A1–A3 EPR centers with neutral, metastable Frenkel pairs involving chemical reconstructions.

VI. CONCLUSIONS

In summary, we have presented evidence that the formation of metastable Frenkel-pair configurations can explain a range of observations in Ib diamond. In particular, this model for the W11–W14 EPR centers has the advantage over the previous compressed vacancy model in that it can explain why there are exactly four distinct structures of specific symmetries, displays an energy variation which allows for correlation of the stabilities of the different EPR centers with temperature, and fits with the experimental annealing barriers.[37] Moreover, in nitrogen-lean material, Frenkel pairs are only stable in three configurations, in line with a tentative assignment with the A1–A3 EPR centers in this type of material.

If these assignments are correct, this is additional evidence, along with the formation of metastable self-interstitial complexes, $I\cdots N_s$, and $N_i\cdots N_s$ complexes of the persistence of metastable configurations to relatively high temperatures in diamond, all of which rely on the propensity of carbon to form reconstructions including those involving π bonds.

Finally, it is clear from the electronic structure of Frenkel pairs, both with and without nitrogen directly incorporated into the defect, that one would expect a range of optical and vibrational systems to be produced in irradiated type Ib diamond. In a previous paper,[10] it was proposed that the transient optical absorption seen in this type of material may be assigned to metastable $I\cdots N_s$ or $N_i\cdots N_s$ pairs due to the detection of LVM replica to the zero-phonon transitions. However, one or more of the experimental centers investigated in the previous study may relate to Frenkel-pair defects.

ACKNOWLEDGMENTS

We gratefully acknowledge useful discussions with R. Jones, School of Physics, University of Exeter UK. J.P.G., P.R.B., and M.J.R. also acknowledge the EPSRC for funding.

[1] G. Davies, S. C. Lawson, A. T. Collins, A. Mainwood, and S. J. Sharp, Phys. Rev. B **46**, 13157 (1992).
[2] J. Isoya, H. Kanda, Y. Uchida, S. C. Lawson, S. Yamasaki, H. Itoh, and Y. Morita, Phys. Rev. B **45**, 1436 (1992).
[3] J. P. Goss, B. J. Coomer, R. Jones, T. D. Shaw, P. R. Briddon, M. Rayson, and S. Öberg, Phys. Rev. B **63**, 195208 (2001).
[4] H. E. Smith, G. Davies, M. E. Newton, and H. Kanda, Phys. Rev. B **69**, 045203 (2004).
[5] D. C. Hunt, D. J. Twitchen, M. E. Newton, J. M. Baker, T. R. Anthony, W. F. Banholzer, and S. S. Vagarali, Phys. Rev. B **61**, 3863 (2000).
[6] D. J. Twitchen, D. C. Hunt, M. E. Newton, J. M. Baker, T. R. Anthony, and W. F. Banholzer, Physica B **273-274**, 628 (1999).
[7] M. E. Newton, B. A. Campbell, D. J. Twitchen, J. M. Baker, and T. R. Anthony, Diamond Relat. Mater. **11**, 618 (2002).
[8] D. J. Twitchen, M. E. Newton, J. M. Baker, O. D. Tucker, T. R. Anthony, and W. F. Banholzer, Phys. Rev. B **54**, 6988 (1996).
[9] J. P. Goss, R. Jones, and P. R. Briddon, Phys. Rev. B **65**, 035203 (2002).
[10] J. P. Goss, P. R. Briddon, S. Papagiannidis, and R. Jones, Phys. Rev. B **70**, 235208 (2004).
[11] C. P. Ewels, R. H. Telling, A. A. El-Barbary, M. I. Heggie, and P. R. Briddon, Phys. Rev. Lett. **91**, 025505 (2003).
[12] R. Jones and P. R. Briddon, in *Identification of Defects in Semiconductors*, Semiconductors and Semimetals, Vol. 51A, edited by M. Stavola (Academic, Boston, 1998), Chap. 6.
[13] H. J. Monkhorst and J. D. Pack, Phys. Rev. B **13**, 5188 (1976).
[14] C. Hartwigsen, S. Goedecker, and J. Hutter, Phys. Rev. B **58**, 3641 (1998).
[15] J. P. Goss, M. J. Shaw, and P. R. Briddon, in *Theory of Defects in Semiconductors*, Topics in Applied Physics, Vol. 104, edited by David A. Drabold and Stefan K. Estreicher (Springer, Berlin, 2007), pp. 69–94.
[16] D. A. Liberman, Phys. Rev. B **62**, 6851 (2000).
[17] G. Makov and M. C. Payne, Phys. Rev. B **51**, 4014 (1995).
[18] J.-W. Jeong and A. Oshiyama, Phys. Rev. B **64**, 235204 (2001).
[19] J. P. Goss, P. R. Briddon, S. J. Sque, and R. Jones, Diamond Relat. Mater. **13**, 684 (2004).
[20] M. J. Rayson, J. P. Goss, and P. R. Briddon, Physica B **340-342**, 673 (2003).
[21] R. Jones, P. R. Briddon, and S. Öberg, Philos. Mag. Lett. **66**, 67 (1992).
[22] R. Q. Hood, P. R. C. Kent, R. J. Needs, and P. R. Briddon, Phys. Rev. Lett. **91**, 076403 (2003).
[23] U. von Barth, Phys. Rev. A **20**, 1693 (1979).
[24] S. J. Breuer and P. R. Briddon, Phys. Rev. B **51**, 6984 (1995).
[25] J. P. Goss, R. Jones, S. J. Breuer, P. R. Briddon, and S. Öberg, Phys. Rev. Lett. **77**, 3041 (1996).

[26] J. P. Goss, P. R. Briddon, M. J. Rayson, S. J. Sque, and R. Jones, Phys. Rev. B **72**, 035214 (2005).
[27] F. Cargnoni, C. Gatti, and L. Colombo, Phys. Rev. B **57**, 170 (1998).
[28] G. Davies, C. Foy, and K. O'Donnell, J. Phys. C **14**, 4153 (1981).
[29] A. T. Collins and P. M. Spear, J. Phys. C **19**, 6845 (1986).
[30] A. T. Collins, P. J. Woad, G. S. Woods, and H. Kanda, Diamond Relat. Mater. **2**, 136 (1993).
[31] J. W. Steeds, T. J. Davis, S. J. Charles, J. M. Hayes, and J. E. Butler, Diamond Relat. Mater. **8**, 1847 (1999).
[32] L. Allers, A. T. Collins, and J. Hiscock, Diamond Relat. Mater. **7**, 228 (1998).
[33] D. J. Twitchen, D. C. Hunt, C. Wade, M. E. Newton, J. M. Baker, T. R. Anthony, and W. F. Banholzer, Physica B **273-274**, 644 (1999).
[34] J. E. Lowther and J. A. van Wyk, Phys. Rev. B **49**, 11010 (1994).
[35] O. D. Tucker, M. E. Newton, J. M. Baker, and J. A. van Wyk, Diamond Conference, Bristol 1993 (unpublished).
[36] J. van Wyk and G. Woods, Diamond Conference, Oxford, 1987 (unpublished).
[37] G. F. Flynn, J. A. van Wyk, and M. J. R. Hoch, Diamond Conference, Reading, 1990 (unpublished).
[38] K. Iakoubovskii, S. Dannefaer, and A. Stesmans, Phys. Rev. B **71**, 233201 (2005).
[39] S. Dannefaer, A. Pu, and D. Kerr, Diamond Relat. Mater. **10**, 2113 (2001).
[40] R. Farrer, Solid State Commun. **7**, 685 (1969).
[41] A. Mainwood, J. E. Lowther, and J. A. van Wyk, J. Phys.: Condens. Matter **5**, 7929 (1993).
[42] W. V. Smith, P. P. Sorokin, I. L. Gelles, and G. J. Lasher, Phys. Rev. **115**, 1546 (1959).
[43] Y. M. Kim and G. D. Watkins, J. Appl. Phys. **42**, 722 (1971).
[44] Y. M. Kim, Y. H. Lee, P. Brosious, and J. W. Corbett, *Radiation Damage and Defects in Semiconductors*, Institute of Physics Conference Series No. 16 (Institute of Physics, London, 1972), pp. 202–209.
[45] C. A. Coulson and M. J. Kearsley, Proc. R. Soc. London, Ser. A **241**, 433 (1957).
[46] C. A. J. Ammerlaan, in *Semiconductors, Impurities and Defects in Group IV Elements and III-V Compounds*, Landolt-Börnstein, New Series, Vol. III41A2α edited by M. Schultz (Springer, Berlin, 2002).